IEEE Photonics Journal
An IEEE Photonics Society Publication

Analysis of Quantum-Dot Spin-VCSELs

Volume 4, Number 4, August 2012

Mike J. Adams
Dimitris Alexandropoulos

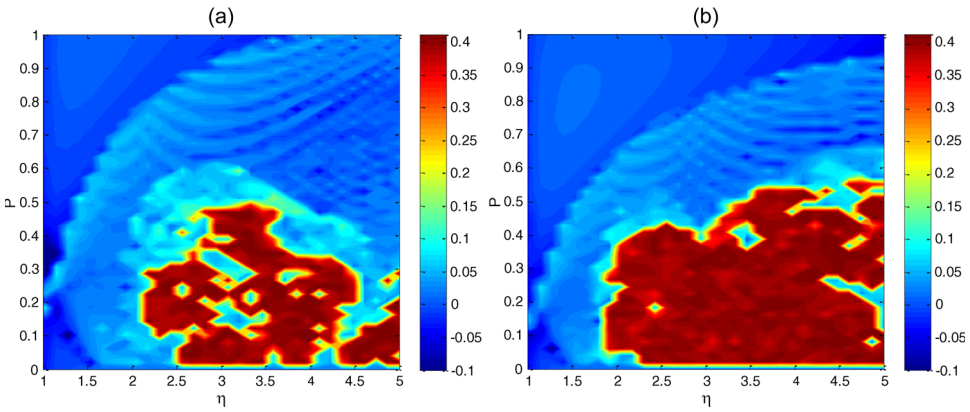

DOI: 10.1109/JPHOT.2012.2204868
1943-0655/$31.00 ©2012 IEEE

Analysis of Quantum-Dot Spin-VCSELs

Mike J. Adams[1] **and Dimitris Alexandropoulos**[1,2]

[1]School of Computer Science and Electronic Engineering, University of Essex, Colchester, CO4 3SQ, U.K.
[2]Department of Materials Science, University of Patras, 26504 Rio, Greece

DOI: 10.1109/JPHOT.2012.2204868
1943-0655/$31.00 ©2012 IEEE

Manuscript received May 23, 2012; revised June 11, 2012; accepted June 11, 2012. Date of publication June 14, 2012; date of current version June 29, 2012. This work was supported by the U.K. Engineering and Physical Sciences Research Council (EPSRC) under Grant EP/H00873X/1. Corresponding author: M. J. Adams (e-mail: adamm@essex.ac.uk).

Abstract: The derivation of a set of rate equations (REs) to describe optically pumped quantum-dot (QD) spin-injected vertical-cavity surface-emitting lasers (VCSELs) is presented based on a modified version of the spin-flip model. The approach includes capture of spin-up and spin-down electrons from the wetting layer into the ground state of the QD and also coupling between left- and right-circularly polarized fields caused by birefringence and dichroism. Numerical solutions of the REs are presented in the form of stability maps in the plane of pump polarization and total pump intensity; examples of calculated time series of the polarized field components are also given for specific cases of interest. The values of the spin-relaxation rate, the carrier capture rate, and the gain parameter are shown to have a significant effect on the dynamics of quantum-dot spin-VCSELs.

Index Terms: Quantum dots, semiconductor lasers, vertical cavity surface emitting lasers, optical polarization, nonlinear dynamical systems, chaos.

1. Introduction

Optoelectronic devices with spin-polarized carriers offer the possibility of output polarization control. Lasers whose output polarization can be controlled are already of interest as sources for quantum computing and cryptography, in chemistry and biology for studying molecules exhibiting optical activity, and in a growing list of other areas. The operation principle relies on the coupling of spin-up(down) electrons to the left(right)-circularly polarized optical field in a quantized system. The challenge in such devices is the injection of spin-polarized carriers with an enhanced spin lifetime at room temperature. Two routes for spin injection have been researched: electrical injection with magnetic contacts [1] and optical pumping [2]. Spin optoelectronics research has been fueled by recent demonstrations of an electrically injected quantum-dot (QD) spin-vertical-cavity surface-emitting laser (VCSEL) operating at 200 K [3], an optically pumped spin-VCSEL grown on a (110) substrate [4], and optical pumping of a dilute nitride spin-VCSEL [5]. Despite the significance of these demonstrations, the ultimate challenge that spin optoelectronics research faces is the realization of electrically injected spin devices with an enhanced spin lifetime operating at room temperature.

Modeling of spin-VCSELs usually employs a rate-equation (RE) approach that accounts for the dynamics and coupling of spin polarizations [6]–[10]. The spin-flip model [8]–[10] (SFM) is a convenient formulation of the RE for VCSELs that is most commonly used. In the context of the SFM, the carrier populations in the conduction band and valence band (VB) are grouped in two distinct carrier densities on the basis of their spin property, i.e., spin-up and spin-down. Lasing transitions associated with these carrier densities produce left- or right-handed circularly polarized

light. The spin-up and spin-down carrier populations are coupled via the spin-flip process that takes place with a characteristic time described by the inverse of the spin-relaxation rate (γ_s). The SFM also accounts for the coupling between the circularly polarized modes of the VCSEL via the effects of gain anisotropy or dichroism (i.e., different gain for the two modes) and birefringence (i.e., different refractive index for the two modes) described with rates γ_a and γ_p, respectively. The SFM has been used to model optically pumped VCSELs [5], [11] and VCSELs with electrical spin injection [12], [13] with an appropriate modification of the pumping term.

Various levels of refinement of the RE model have been reported in the literature. These include simplified approaches where dichroism and birefringence are neglected [1], [7], [11]–[16], incorporation of transitions from the barrier into the quantum well (QW) [15], [16], and modification of the SFM under the assumption that the two circularly polarized field components have the same frequency and maintain a constant phase difference [17], [18]. Recently, we have reported a comprehensive study on the dynamic properties of optically pumped VCSELs [19] that used the full SFM (with no simplifying assumptions) in combination with the largest Lyapunov exponent (LLE) to identify different dynamics (stability, periodicity, and chaos).

While spin-VCSELs with QW gain regions have dominated the research activity, recent reports have diverted interest toward VCSELs that incorporate QD gain regions [1], [3], [13], [20]. Research in QD spin-VCSELs is motivated by the well-established advantages of QDs for conventional VCSELs that include temperature-tolerant performance, excitonic gain, suppression of carrier diffusion, and design flexibility. Most relevant to QD spin-VCSELs is the possibility for a long spin-relaxation rate by virtue of the spatial localization of carriers in the QDs that inhibits the D'yakonov–Perel spin scattering process and phonon scattering, both of which tend to reduce the spin lifetime [21].

QD spin-VCSELs have been modeled using a simplified model that includes transitions from the wetting layer (WL) to the dot levels but neglects birefringence and gain anisotropy [1], [6], [12], [13], [20]. In a recent report [22], we have presented the first (to our knowledge) stability analysis of optically pumped QD spin-VCSELs that used a modified SFM to present contours of output polarization and output total intensity in the plane of pump polarization and total pump intensity. In the present contribution, we derive the modified SFM applicable to optically pumped QD spin-VCSELs and proceed to study the dynamics using the LLE method as a gauge for the dynamic behavior. The rest of this paper is organized as follows. In Section 2, we present a detailed derivation of the SFM equations for QD spin-VCSELs. We begin with the derivation of the un-normalized SFM equations and then introduce the appropriate normalization that permits comparison with the SFM for the QW case. The conditions under which the QD SFM converges to the QW SFM are investigated in Section 3. In Section 4, with the aid of the LLE method, we explore the effect of SFM parameters and other parameters relevant to QDs on the dynamics of QD spin-VCSELs.

2. Theoretical Model

Ignoring spin effects, the operation of a QD-VCSEL can be described by the solution of the REs for the carrier dynamics and the field RE [23]. The scope of the present contribution is to introduce spin effects into the QD-VCSEL theoretical formalism, by combining the spinless REs with the key aspects of the SFM model viz., the spin state of carriers, birefringence, and dichroism. The SFM QD-VCSEL model is schematically illustrated in Fig. 1. In order to focus on the key effects related to spin and polarization, excited states of the QDs are neglected in our approach. Optical pumping produces carriers with spin-up and spin-down (denoted by superscripts $-$ and $+$, respectively) in the WL, and the spin-relaxation process between these carrier populations is characterized by a rate γ_{WLs}. These carriers are also captured into the ground state (GS) of the dots at a rate γ_o to produce carrier populations with spin-up and spin-down. Lasing occurs via transitions from the GS to the VB, and the resulting left- and right-circularly polarized electric fields are coupled by birefringence at a rate γ_p. Coupling via dichroism at a rate γ_a also occurs but is not explicitly shown in Fig. 1. In the following, we detail the derivation of the modified SFM equations based on the model in Fig. 1.

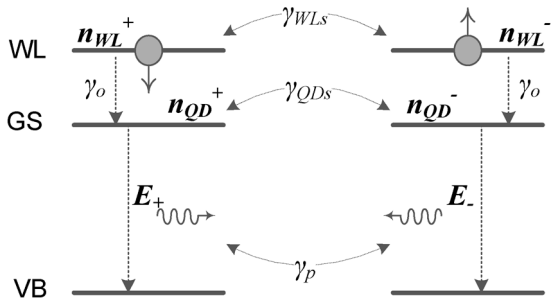

Fig. 1. Six-level system used for the SFM in a QD spin-VCSEL [22]. The WL, GS, and VB energy levels are depicted.

2.1. REs for the Case When Spin Is Neglected

The material gain per unit length, i.e., g_m, for a QD medium has an excitonic form

$$g_m = aN_{QD}(2f_{GS} - 1) \tag{1}$$

where a is the differential gain, N_{QD} is the density of dots per volume, and f_{GS} is the occupation probability of the GS. Then, the RE for the complex electric field, i.e., E_o, can be written as

$$\frac{dE_o}{dt} = \frac{v_g}{2}\left[\Gamma aN_{QD}(2f_{GS} - 1) - \frac{1}{v_g\tau_p}\right]E_o + i\omega E_o \tag{2}$$

where v_g is the group velocity, Γ is the optical confinement factor, τ_p is the photon lifetime, and ω is the lasing angular frequency. Now, define the cavity loss rate $\kappa = (2\tau_p)^{-1}$ and the normalized gain coefficient $h = v_g\Gamma aN_{QD}\tau_p$, so that (2) becomes

$$\frac{dE_o}{dt} = \kappa[h(2f_{GS} - 1) - 1]E_o + i\omega E_o. \tag{3}$$

If the angular frequency at threshold is ω_o, then, to a good approximation, the oscillating field's angular frequency can be expressed as

$$\omega = \omega_o + \alpha\kappa[h(2f_{GS} - 1) - 1] \tag{4}$$

where α is the linewidth enhancement factor. Hence, (3) can be written in the form

$$\frac{dE_o}{dt} = \kappa[h(2f_{GS} - 1) - 1](1 + i\alpha)E_o + i\omega_o E_o. \tag{5}$$

The angular frequency can be eliminated by writing

$$E_o = E\exp(i\omega_o t) \tag{6}$$

so that (5) now assumes the conventional form

$$\frac{dE}{dt} = \kappa[h(2f_{GS} - 1) - 1](1 + i\alpha)E. \tag{7}$$

For the carrier REs, following the approach in [24] and in [20, Sec. 3], we make the simplifying assumption that recombination occurs only by transitions from the GS and not from the WL. Paoli blocking of states in the WL is omitted, and carrier escape from the QD to the WL is neglected. Thus, electrons injected into the WL can only be captured into the GS, and the RE for the WL occupation probability f_{WL} is

$$\frac{df_{WL}}{dt} = \frac{I}{eN_{WL}} - \gamma_o f_{WL}(1 - f_{GS}) \tag{8}$$

where I is the rate of injection per unit volume (by current in conventional VCSELs or by optical pumping in the case considered here), e is the electron charge, and N_{WL} is the density of states in the WL. Electrons captured into the GS can either recombine nonradiatively or via spontaneous or stimulated emission with holes in the QD VB states. Hence, the RE is

$$\frac{df_{GS}}{dt} = \gamma_o f_{WL} \frac{N_{WL}}{N_{QD}} (1 - f_{GS}) - \gamma_n f_{GS} - v_g \Gamma a (2 f_{GS} - 1) |E|^2 \tag{9}$$

where γ_n is the recombination rate.

2.2. REs Including Spin

Spin can be introduced now in a straightforward manner by accounting for the polarized fields $E_{\pm}$, where the subscript $+(-)$ denotes right(left)-circular polarization, and their coupling via dichroism (not shown in Fig. 1) and birefringence:

$$\frac{dE_{\pm}}{dt} = \kappa \left[h\left(2 f_{GS}^{\pm} - 1\right) - 1 \right] (1 + i\alpha) E_{\pm} - (\gamma_a + i\gamma_p) E_{\mp} \tag{10}$$

where γ_a and γ_p are the rates of dichroism and birefringence, respectively, and $f_{GS}^{\pm}$ is the occupation probability of the GS with spin-up (superscript $-$) or spin-down (superscript $+$).

Likewise, spin can be introduced in the carrier REs (8) and (9) by accounting for the spin-polarized carriers, with occupation probabilities $f_{WL}^{\pm}$ for the WL, and the spin-injection rates $I^{\pm}$. If we make the assumption that the spin-relaxation rates are the same for the WL and the GS, denoted by γ_j, then the REs are

$$\frac{df_{WL}^{\pm}}{dt} = \frac{I^{\pm}}{eN_{WL}} - \gamma_o f_{WL}^{\pm} \left(1 - f_{GS}^{\pm}\right) \mp \gamma_j \left(f_{WL}^{+} - f_{WL}^{-}\right) \tag{11}$$

$$\frac{df_{GS}^{\pm}}{dt} = \gamma_o f_{WL}^{\pm} \frac{N_{WL}}{N_{QD}} \left(1 - f_{GS}^{\pm}\right) - \gamma_n f_{GS}^{\pm} - v_g \Gamma a \left(2 f_{GS}^{\pm} - 1\right) |E_{\pm}|^2 \mp \gamma_j \left(f_{GS}^{+} - f_{GS}^{-}\right). \tag{12}$$

2.3. Normalization of Spin QD-VCSEL Equations

The transformation of (10)–(12) to normalized forms can be made by the following changes of variable:

$$n_{GS}^{\pm} = h\left(2 f_{GS}^{\pm} - 1\right) \tag{13}$$

$$n_{WL}^{\pm} = h \frac{N_{WL}}{N_{QD}} f_{WL}^{\pm} \tag{14}$$

$$\eta^{\pm} = \frac{1}{2} \frac{I^{\pm} - I_{transp}^{\pm}}{I_{th}^{\pm} - I_{transp}^{\pm}} \tag{15}$$

$$E_{s\pm} = E_{\pm} \sqrt{\frac{v_g \Gamma a}{\gamma_n}} \tag{16}$$

where $\eta_{\pm}$ is the normalized pumping term, $E_{s\pm}$ is the normalized polarized field, and $I_{th}^{\pm}$ and $I_{transp}^{\pm}$ are the carrier injection components at threshold and transparency, respectively, for linear polarization. Expressions for these can be found by applying the threshold and transparency conditions, respectively, to the steady-state solution of (11). Applying the threshold condition $h(2f_{GS}^{\pm} - 1) = 1$, the value of the WL occupation probability at threshold for linear polarization ($f_{GS}^{+} = f_{GS}^{-}, f_{WL}^{+} = f_{WL}^{-}$) is found from the steady-state solution of (12):

$$f_{WL}^{\pm}\big|_{th} = \frac{\gamma_n}{\gamma_o} \frac{N_{QD}}{N_{WL}} \frac{h+1}{h-1}. \tag{17}$$

Substituting this result in (11) yields an expression for the threshold current

$$\frac{I_{th}^{\pm}}{e} = \gamma_n N_{QD} \frac{h+1}{2h}. \tag{18}$$

Likewise, applying the transparency condition $(f_{GS} = 0.5)$ yields

$$f_{WL}^{\pm}\big|_{transp} = \frac{\gamma_n}{\gamma_o}\frac{N_{QD}}{N_{WL}} \tag{19}$$

$$\frac{I_{transp}^{\pm}}{e} = \frac{\gamma_n}{2} N_{QD}. \tag{20}$$

Using (18) and (20) in (15) gives

$$\frac{I^{\pm}}{e} = N_{QD}\gamma_n\left(\frac{1}{2} + \frac{\eta^{\pm}}{h}\right). \tag{21}$$

Using (13), (14), (16), and (21), the normalized REs are

$$\frac{dE_{s\pm}}{dt} = \kappa\left(n_{GS}^{\pm} - 1\right)(1 + i\alpha)E_{s\pm} - (\gamma_a + i\gamma_p)E_{s\mp} \tag{22}$$

$$\frac{dn_{WL}^{\pm}}{dt} = \eta^{\pm}\gamma_n + h\frac{\gamma_n}{2} - \gamma_o n_{WL}^{\pm}\left[\frac{h - n_{GS}^{\pm}}{2h}\right] \mp \gamma_j\left(n_{WL}^{+} - n_{WL}^{-}\right) \tag{23}$$

$$\frac{dn_{GS}^{\pm}}{dt} = \gamma_o\frac{n_{WL}^{\pm}}{h}\left(h - n_{GS}^{\pm}\right) - \gamma_n\left(h + n_{GS}^{\pm}\right) \mp \gamma_j\left(n_{GS}^{+} - n_{GS}^{-}\right) - 2\gamma_n n_{GS}^{\pm}|E_{s\pm}|^2. \tag{24}$$

Equations (22)–(24) provide the necessary theoretical framework for the description of spin-polarized QD-VCSELs.

3. Validation of the Modified SFM Equations

The modified SFM model for the description of QD spin-VCSELs is consistent with the other treatments of QD spin-VCSELs [1], [6], [12], [13], [20], despite the differences in the details of the assumptions made. The difference from the QW SFM model is the inclusion of the WL (23) that is coupled with the GS (24) via the carrier relaxation rate. In the limit when the capture of carriers from the WL to the GS is instantaneous, i.e., $(\gamma_o \to \infty)$, then $n_{WL}^{\pm} = 0$ and (24) transforms to that of QW case. To show this, consider the limit of $\gamma_o \to \infty$, $dn_{WL}^{\pm}/dt = 0$, $n_{WL}^{\pm} = 0$, when (23) becomes

$$2\eta^{\pm}\gamma_n + h\gamma_n - \gamma_o n_{WL}^{\pm}\left[\frac{h - n_{GS}^{\pm}}{h}\right] = 0. \tag{25}$$

Adding (25) and (24) yields

$$\left.\frac{dn_{GS}^{\pm}}{dt}\right|_{\gamma_o\to\infty} = 2\eta^{\pm}\gamma_n - \gamma_n n_{GS_{\gamma_o\to\infty}}^{\pm} \mp \gamma_j\left(n_{GS_{\gamma_o\to\infty}}^{+} - n_{GS_{\gamma_o\to\infty}}^{-}\right) - 2\gamma_n n_{GS_{\gamma_o\to\infty}}^{\pm}|E_{s\pm}|_{\gamma_o\to\infty}^{2}. \tag{26}$$

Equation (26) is identical with the well-known corresponding equation for the QW spin-VCSEL (see, e.g., [19] and references therein).

An additional validity test concerns the relation between the total emitted intensity and the normalized optical pump rate. In the steady state for linear polarization, $n_{GS}^{\pm} = 1$, $E_{+} = E_{-}$, $\eta^{+} = \eta^{-}$,

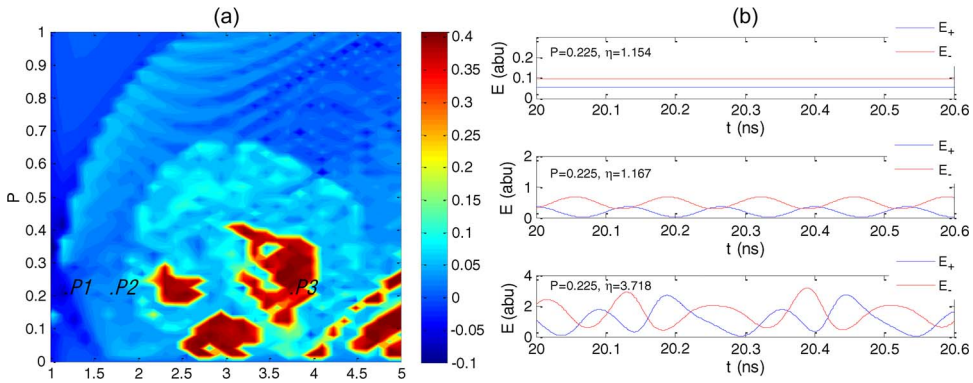

Fig. 2. (a) Stability map in the P, η plane of a QD spin-VCSEL for the following set of parameters: $h = 1.1995$, $\gamma_o = 400\ \text{ns}^{-1}$, $\gamma_j = 10\ \text{ns}^{-1}$, $\gamma_p = 20\ \text{ns}^{-1}$, $\gamma_a = 0$, $\gamma_n = 1\ \text{ns}^{-1}$, $\kappa = 250\ \text{ns}^{-1}$, and $\alpha = 3$. (b) Time traces for the points $P1$ $(P = 0.225, \eta = 1.154)$, $P2$ $(P = 0.225, \eta = 1.167)$, and $P3$ $(P = 0.225, \eta = 3.718)$ of (a).

and (24) and (23), respectively, give

$$\gamma_o n_{WL}^{+}\left(\frac{h-1}{2h}\right) = \gamma_n \frac{(h+1)}{2} + \gamma_n |E_{s+}|^2 \tag{27}$$

$$\eta^{+}\gamma_n + h\frac{\gamma_n}{2} = \gamma_o n_{WL}^{+}\left[\frac{h-1}{2h}\right]. \tag{28}$$

Substituting (27) into (28) gives the result

$$2\eta^{+} - 1 = 2|E_{+}|^2. \tag{29}$$

This is identical with the corresponding result for the QW case [9] and can be expressed in terms of the total normalized pump rate η as

$$\eta = \eta^{+} + \eta^{-} = 1 + |E_{+}|^2 + |E_{-}|^2. \tag{30}$$

4. Results and Discussion

Equations (22)–(24) have been numerically solved to map the dynamic behavior of the QD spin-VCSEL in the plane of pump polarization (ellipticity) P, defined as $P = (\eta_{+} - \eta_{-})/(\eta_{+} + \eta_{-})$, and total pump intensity η, defined as in (30). Since the results are symmetric about $P = 0$, only positive values of P are plotted in what follows. The dynamics are characterized using the LLE method previously used [19]. Discrimination between the dynamics is made on the basis of the value of the LLE: negative values correspond to stability, zero corresponds to oscillatory behavior, whereas positive values correspond to complex dynamics that tend toward chaotic behavior as the LLE increases. Fig. 2(a) shows the stability map in the (P, η) plane of a QD spin-VCSEL for the following set of parameters: $h = 1.1995$, $\gamma_o = 400\ \text{ns}^{-1}$, $\gamma_j = 10\ \text{ns}^{-1}$, $\gamma_o = 400\ \text{ns}^{-1}$, $\gamma_p = 20\ \text{ns}^{-1}$, $\gamma_a = 0$, $\gamma_n = 1\ \text{ns}^{-1}$, $\kappa = 250\ \text{ns}^{-1}$, and $\alpha = 3$. The contours of LLE values in Fig. 2(a) are defined on the color scale that gives the LLE value. Fig. 2(b) shows indicative time traces of stability, oscillatory and more complex dynamics for points $P1$, $P2$, and $P3$ in Fig. 2(a).

The QD spin-VCSEL exhibits an enhanced broad unstable region with complex dynamic behavior for a wide range of $P - \eta$ values. The results from the modified SFM are to be compared with previous work on QW spin-VCSELs [19], [25]. Despite the fact that a strict comparison is not possible for the two cases for reasons to be explained later on, it is notable that regions of chaotic and more complex dynamics are relatively small compared with the QW counterpart. Additionally, the maximum values of LLE calculated for QD spin-VCSELs are smaller than the ones for the QW spin-VCSEL, suggesting a less complicated unstable dynamics for the case of QDs.

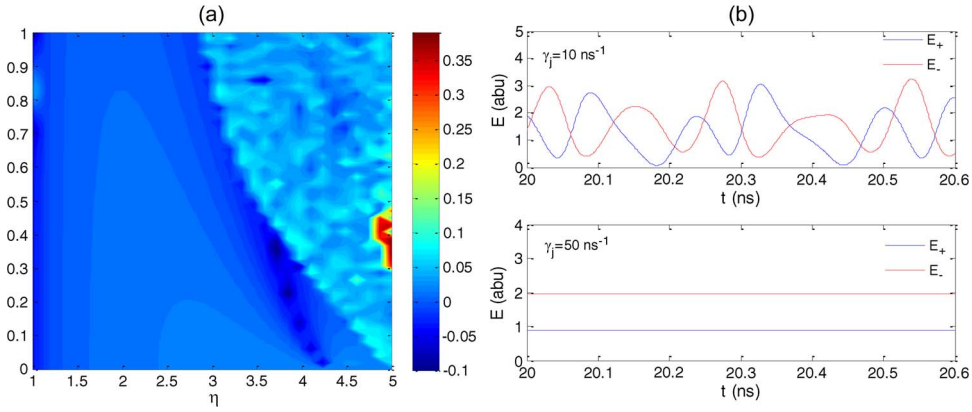

Fig. 3. (a) Stability map in the P, η plane of a QD spin-VCSEL for $h = 1.1995$, $\gamma_j = 50$ ns^{-1}, and the rest of the SFM parameters the same as in Fig. 2. (b) Time traces for $P = 0.265$, $\eta = 3.846$ for $\gamma_j = 10$ ns^{-1} and $\gamma_j = 50$ ns^{-1}.

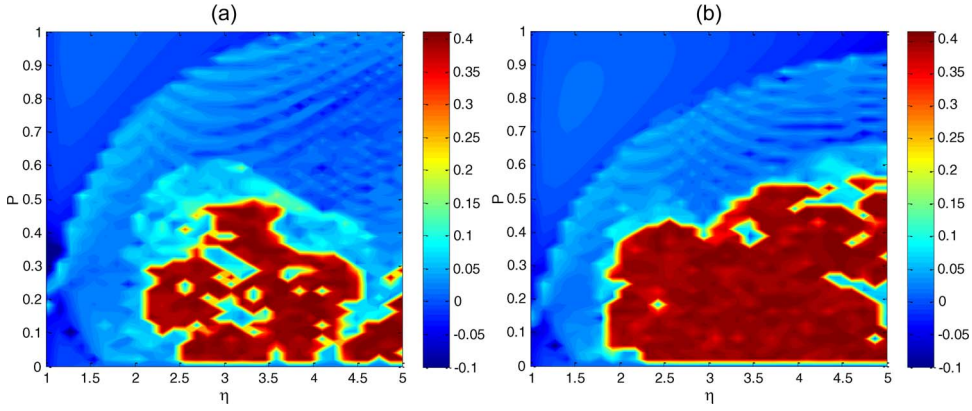

Fig. 4. (a) Stability map in the P, η plane of a QD spin-VCSEL for the following set of parameters: $h = 1.1995$ and $\gamma_o = 600$ ns^{-1}, with the other parameters the same as in Fig. 2. (b) Stability map for $h = 1.665$, with the rest of the parameters the same as in (a).

The reduced dimensionality of the QD permits the tailoring of the spin-relaxation time. Hence, it is instructive to explore the effect of γ_s on the dynamics of a QD spin-VCSEL. We do so in Fig. 3 where, again, the dynamics are identified with the aid of LLE in the $P - \eta$ plane.

Acceleration of the spin relaxation results in extended stability and suppression of the region of more complex dynamics for this specific set of SFM parameters. A similar result has been recently calculated for QW spin-VCSELs [19]. Fig. 3(b) shows the transition from nearly chaotic dynamics to stability for the point $(P, \eta) = (0.265, 3.846)$ in the stability maps of Figs. 2(a) and 3(a).

Parameters γ_o and h are specific to QD spin-VCSELs and combine the QD effects. Fig. 4 depicts the effect of increasing gain parameter h on the dynamics of the QD spin-VCSEL.

While the region of instability is reduced with an increase of the gain parameter h, the resulting unstable region is characterized by more complex dynamics. It is desirable from a device point of view for the h parameter to be tuned to the application's requirements. Recalling the expression $h = v_g \Gamma a N_{QD} \tau_p$, the gain parameter h groups the material (aN_{QD}), waveguide $(v_g\Gamma)$, and cavity characteristics (τ_p). One potential tuning scheme of h can be employed using a vertical-external-cavity surface-emitting laser (VECSEL) where the cavity characteristics can be tailored at will. It is worth noting that parameter h, being a convenient lumping of the interplay of material and cavity effects, is indeed a useful design parameter whose applicability is not restricted to spin-polarized

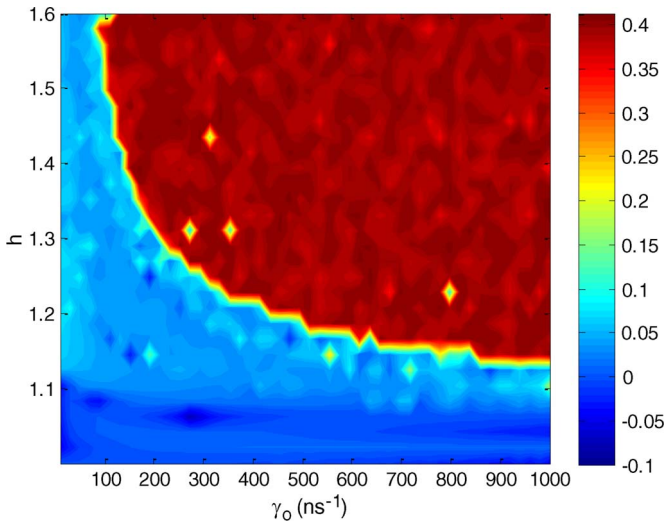

Fig. 5. Stability map in the h, γ_o plane of a QD spin-VCSEL for the following set of parameters: $P = 0.2$, $\eta = 2.2$, $\gamma_j = 10$ ns^{-1}, $\gamma_p = 20$ ns^{-1}, $\gamma_a = 0$, $\gamma_n = 1$ ns^{-1}, $\kappa = 250$ ns^{-1}, and $\alpha = 3$.

QD-VCSELs but extends to conventional QD spin-unpolarized structures such as QD-VCSELs, QD vertical-cavity semiconductor optical amplifiers (VCSOAs) [26], and QD semiconductor optical amplifiers (SOAs) [27].

The effect of γ_o on the stability properties of the VCSEL can be deduced from the comparison of Figs. 2(a) and 4(a). The extent of the unstable region for the given set of SFM parameters is not significantly altered. This is not the case, however, for the complex dynamics where the faster carrier capture from the WL to the GS enhances the chaotic regions of the system.

Evidently, both gain parameters h and γ_o have a substantial effect on the stability properties of the QD spin-VCSEL. This is clearer in Fig. 5 where we explore the dynamics in the plane (h, γ_o) for a given value of P and η $(P = 0.2, \eta = 2.2)$. For a given value of γ_o, variation of h can drive the system from stability to oscillations and, finally, to chaos. The same applies for the case of fixed h and variation of γ_o. It is thus demonstrated that both can be interpreted as additional degrees of freedom for the tailoring and control of the dynamics of QD spin-VCSELs.

The dependence of the stability properties on both h and γ_o makes the comparison with the QW spin-VCSEL difficult. As mentioned above, at the limit $\gamma_o \to \infty$, the QD and the QW converge. However, a formal comparison of the two requires also the appropriate adjustment of parameter h.

5. Conclusion

In this paper, we present a first systematic study of QD spin-VCSEL dynamics in the plane of pump ellipticity versus pump amplitude $(P - \eta)$, using the LLE method with regard to spin-relaxation rate (γ_j) and parameters specific to QDs, i.e., carrier capture rate (γ_o) and gain parameter h. As intuitively expected, variation of γ_j has a profound effect on the dynamics, similar to the effects of spin relaxation for QW spin-VCSELs. Both γ_o and h have a significant effect on the dynamics and can drive the system from stability to oscillatory behavior and to chaos. The regions of chaotic and more complex dynamics of QD spin-VCSELs are smaller compared with the QW spin-VCSELs and also exhibit less complicated unstable dynamics.

Acknowledgment

Prof. I. Henning and Dr. R. Al Seyab are thanked for helpful discussions on the subject of this paper.

References

[1] P. Bhattacharya, D. Basu, A. Das, and D. Saha, "Quantum dot polarized light sources," *Semicond. Sci. Technol.*, vol. 26, no. 1, pp. 014002-1–014002-9, Jan. 2011.

[2] S. Iba, S. Koh, K. Ikeda, and H. Kawaguchi, "Room temperature circularly polarized lasing in an optically spin injected vertical-cavity surface-emitting laser with (110) GaAs quantum wells," *Appl. Phys. Lett.*, vol. 98, no. 8, pp. 081113-1–081113-3, Feb. 2011.

[3] D. Basu, D. Saha, C. C. Wu, M. Holub, Z. Mi, and P. Bhattacharya, "Electrically injected InAs/GaAs quantum dot spin laser operating at 200 K," *Appl. Phys. Lett.*, vol. 92, no. 9, pp. 091119-1–091119-3, Mar. 2008.

[4] H. Fujino, S. Koh, S. Iba, T. Fujimoto, and H. Kawaguchi, "Circularly polarized lasing in a (110)-oriented quantum well vertical-cavity surface-emitting laser under optical spin injection," *Appl. Phys. Lett.*, vol. 94, no. 13, pp. 131108-1–131108-3, Mar. 2009.

[5] K. Schires, R. Al Seyab, A. Hurtado, V.-M. Korpijärvi, M. Guina, I. D. Henning, and M. J. Adams, "Optically-pumped dilute nitride spin-VCSEL," *Opt. Exp.*, vol. 20, no. 4, pp. 3550–3555, Feb. 2012.

[6] M. Holub and P. K. Bhattacharya, "Spin-polarized light-emitting diodes and lasers," *J. Phys. D, Appl. Phys.*, vol. 40, no. 11, pp. R179–R203, Jun. 2007.

[7] C. Gothgen, R. Oszwaldowski, A. Petrou, and I. Zutic, "Analytical model of spin-polarized semiconductor lasers," *Appl. Phys. Lett.*, vol. 93, no. 4, pp. 042513-1–042513-3, Jul. 2008.

[8] M. San Miguel, Q. Feng, and J. V. Moloney, "Light-polarization dynamics in vertical cavity surface-emitting lasers," *Phys. Rev. A*, vol. 52, no. 2, pp. 1728–1739, Aug. 1995.

[9] J. Martin-Regalado, F. Pratl, M. San Miguel, and N. B. Abraham, "Polarization properties of vertical-cavity surface emitting lasers," *IEEE J. Quantum Electron.*, vol. 33, no. 5, pp. 765–783, May 1997.

[10] A. Gahl, S. Balle, and M. San Miguel, "Polarization dynamics of optically pumped VCSELs," *IEEE J. Quantum Electron.*, vol. 35, no. 3, pp. 342–351, Mar. 1999.

[11] S. Hovel, N. Gerhardt, M. Hofmann, J. Yang, D. Reuter, and A. Wieck, "Spin controlled optically pumped vertical cavity surface emitting laser," *Electron. Lett.*, vol. 41, no. 5, pp. 251–253, Mar. 2005.

[12] M. Holub, J. Shin, D. Saha, and P. Bhattacharya, "Electrical spin injection and threshold reduction in a semiconductor laser," *Phys. Rev. Lett.*, vol. 98, no. 14, pp. 146603-1–146603-4, Apr. 2007.

[13] D. Basu, D. Saha, and P. Bhattacharya, "Optical polarization modulation and gain anisotropy in an electrically injected spin laser," *Phys. Rev. Lett.*, vol. 102, no. 12, p. 129 901, Mar. 2009.

[14] J. Lee, W. Falls, R. Oszwaldowski, and I. Zutic, "Spin modulation in semiconductor lasers," *Appl. Phys. Lett.*, vol. 97, no. 4, pp. 041116-1–041116-3, Jul. 2010.

[15] J. Rudolph, D. Hagele, H. M. Gibbs, G. Khitrova, and M. Oestreich, "Laser threshold reduction in a spintronic device," *Appl. Phys. Lett.*, vol. 82, no. 25, pp. 4516–4518, Jun. 2003.

[16] J. Rudolph, S. Dohrmann, D. Hagele, M. Oestreich, and W. Stolz, "Room temperature threshold reduction in vertical cavity surface-emitting lasers by injection of spin-polarized electrons," *Appl. Phys. Lett.*, vol. 87, no. 24, pp. 241117-1–241117-3, Dec. 2005.

[17] A. Dyson and M. J. Adams, "Spin-polarized properties of optically pumped vertical cavity surface emitting lasers," *J. Opt. B, Quantum Semiclass. Opt.*, vol. 5, no. 3, pp. 222–226, Jun. 2003.

[18] M. J. Adams and D. Alexandropoulos, "Parametric analysis of spin-polarized VCSELs," *IEEE J. Quantum Electron.*, vol. 45, no. 6, pp. 744–749, Jun. 2009.

[19] R. K. Al-Seyab, D. Alexandropoulos, I. D. Henning, and M. J. Adams, "Instabilities in spin-polarized vertical-cavity surface-emitting lasers," *IEEE Photon. J.*, vol. 3, no. 5, pp. 799–809, Oct. 2011.

[20] R. Oszwaldowski, C. Gothgen, and I. Zutic, "Theory of quantum dot spin lasers," *Phys. Rev. B, Condens. Matter*, vol. 82, no. 8, pp. 085316-1–085316-7, Aug. 2010.

[21] J. L. Robb, Y. Chen, A. Timmons, K. C. Hall, O. B. Shchekin, and D. G. Deppe, "Time-resolved Faraday rotation measurements of spin relaxation in InGaAs/GaAs quantum dots: Role of excess energy," *Appl. Phys. Lett.*, vol. 90, no. 15, pp. 153118-1–153118-3, Apr. 2007.

[22] D. Alexandropoulos, R. K. Al-Seyab, I. D. Henning, and M. J. Adams, "Instabilities in quantum-dot spin-VCSELs," *Opt. Lett.*, vol. 37, no. 10, pp. 1700–1702, May 2012.

[23] D. O'Brien, S. P. Hegarty, G. Huyet, and A. V. Uskov, "Sensitivity of quantum-dot semiconductor lasers to optical feedback," *Opt. Lett.*, vol. 29, no. 10, pp. 1072–1074, May 2004.

[24] H. D. Summers and P. Rees, "Derivation of a modified Fermi–Dirac distribution for quantum dot ensembles under nonthermal conditions," *J. Appl. Phys.*, vol. 101, no. 7, pp. 073106-1–073106-8, Apr. 2007.

[25] A. Homayounfar and M. J. Adams, "Analysis of SFM dynamics in solitary and optically-injected VCSELs," *Opt. Exp.*, vol. 15, no. 17, pp. 10 504–10 519, Aug. 2007.

[26] M. Vasileiadis, D. Alexandropoulos, M. J. Adams, H. Simos, and D. Syvridis, "Potential of InGaAs/GaAs quantum dots for applications in vertical cavity semiconductor optical amplifiers," *IEEE J. Sel. Topics Quantum Electron.*, vol. 14, no. 4, pp. 1180–1187, Jul./Aug. 2008.

[27] H. C. Wong, G. B. Ren, and J. M. Rorison, "Mode amplification in inhomogeneous QD semiconductor optical amplifiers," *Opt. Quantum Electron.*, vol. 38, no. 4–6, pp. 395–409, Mar. 2006.